

# Tunable charge-transport polarity in thienothiophene-bisoxoindolinylidene-benzodifurandione copolymers for high-performance field-effect transistors

Zhihui Chen,<sup>#ab</sup> Jianyao Huang,<sup>#a</sup> Weifeng Zhang,<sup>\*a</sup> Yankai Zhou,<sup>ab</sup> Xuyang Wei,<sup>ab</sup> Jinbei Wei,<sup>a</sup>

Yuanhui Zheng,<sup>a</sup> Liping Wang,<sup>c</sup> and Gui Yu<sup>\*ab</sup>

<sup>a</sup> *Beijing National Laboratory for Molecular Sciences, CAS Research/Education Center for Excellence in Molecular Sciences, Institute of Chemistry, Chinese Academy of Sciences, Beijing 100190, P. R. China*

*E-mail: zhangwf@iccas.ac.cn, yugui@iccas.ac.cn*

<sup>b</sup> *School of Chemical Sciences, University of Chinese Academy of Sciences, Beijing 100049, P. R. China*

<sup>c</sup> *School of Materials Science and Engineering, University of Science and Technology Beijing, Beijing 100083, P. R. China*

## Contents

1. GPC characterization
2. Thermogravimetric analysis
3. UPS measurements
4. Cyclic voltammetry
5. Theoretical modeling
6. Annealing temperature-dependent mobilities of **PNBDO-TT**
7. Thin film morphology and aggregation characterizations
8. NMR spectra of intermediates and polymers

## 1. GPC characterization

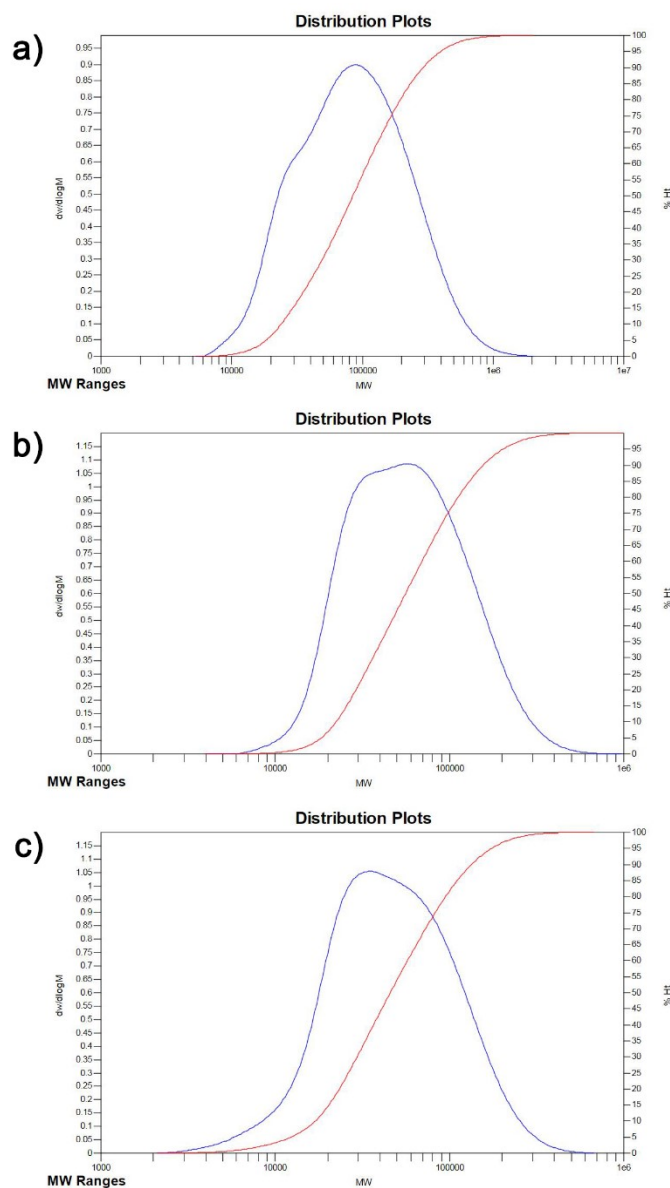


**Fig. S1** High temperature GPC plots of **PNBDO-TT**, **PNBDO-DMTT**, and **PNBDO-MOTT**.

**Table S1** Molecular weights and distribution data extracted from high temperature GPC plots

polymer	$M_p$	$M_n$	$M_v$	$M_w$	$M_z$	$M_{z+1}$	$\bar{D}$
<b>PNBDO-TT</b>	88749	54357	113386	128806	277609	491043	2.3696
<b>PNBDO-DMTT</b>	57162	43665	69156	75295	129269	201157	1.7244
<b>PNBDO-MOTT</b>	35061	32462	57315	62940	111681	173678	1.9389

## 2. Thermogravimetric analysis

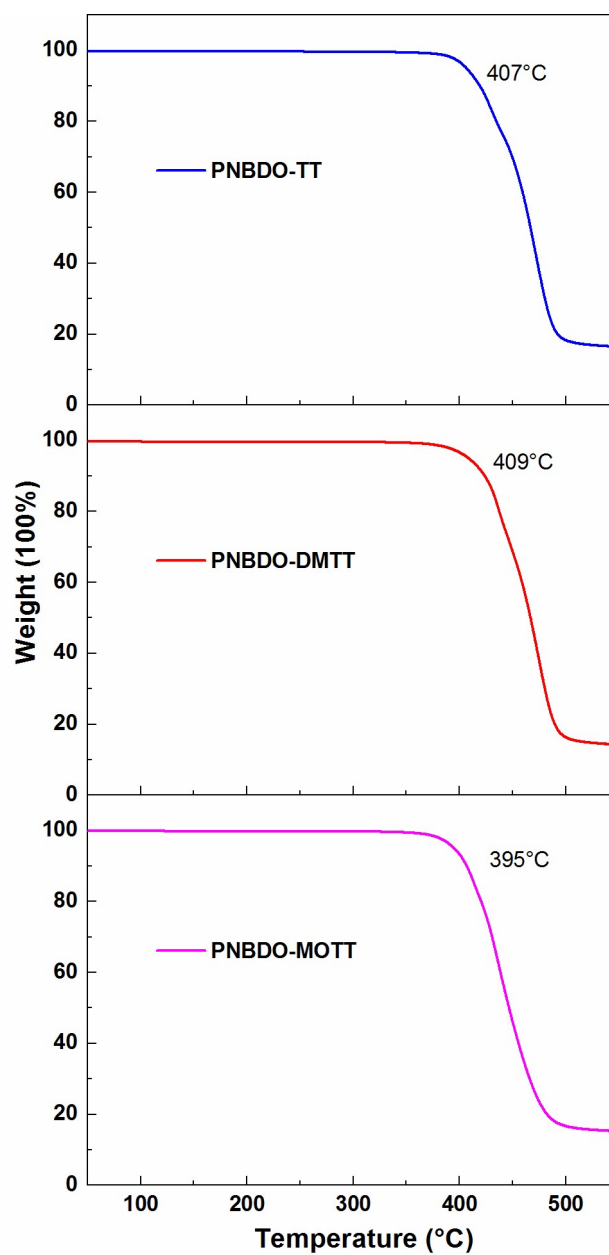


**Fig. S2** TGA traces of **PNBDO-TT**, **PNBDO-DMTT**, and **PNBDO-MOTT**. The inset values are their respective  $T_{dec}$  of three polymers.

## 3. UPS measurements

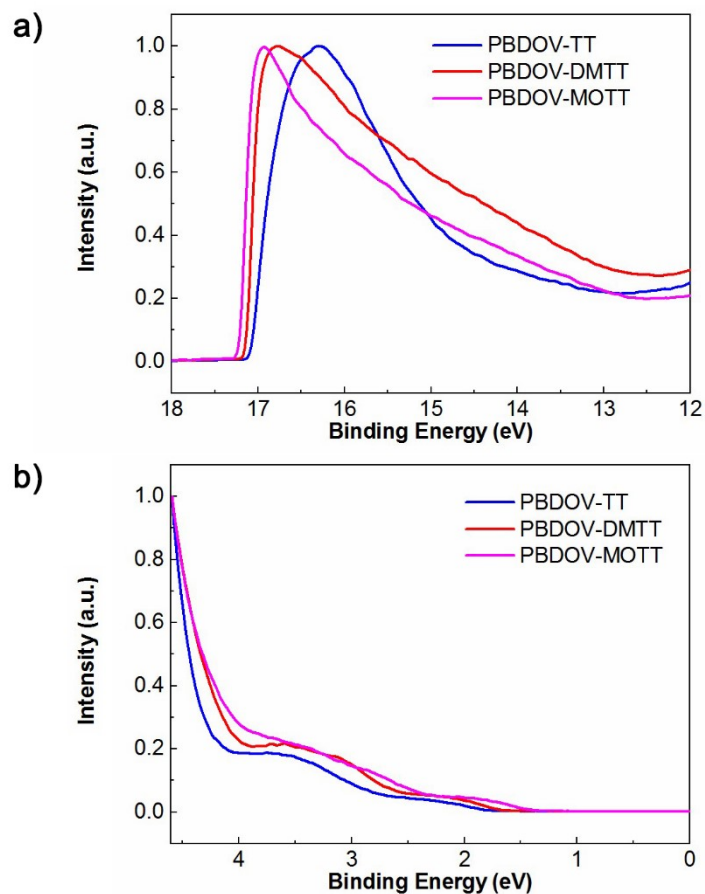


**Fig. S3** UPS spectra of **PNBDO-TT**, **PNBDO-DMTT**, and **PNBDO-MOTT** thin films: (a) secondary electron cutoff spectra and (b) valence band spectra.

**Table S2** UPS Parameters of **PNBDO-TT**, **PNBDO-DMTT**, and **PNBDO-MOTT**

polymer	$E_{\text{cutoff}}$ (eV)	$E_{\text{H, onset}}$ (eV)	IP (eV)	$E_{\text{HOMO}}^{\text{UPS}}$ (eV)
<b>PNBDO-TT</b>	17.08	1.78	5.92	−5.92
<b>PNBDO-DMTT</b>	17.15	1.65	5.72	−5.72
<b>PNBDO-MOTT</b>	17.22	1.41	5.41	−5.41

#### 4. Cyclic voltammetry

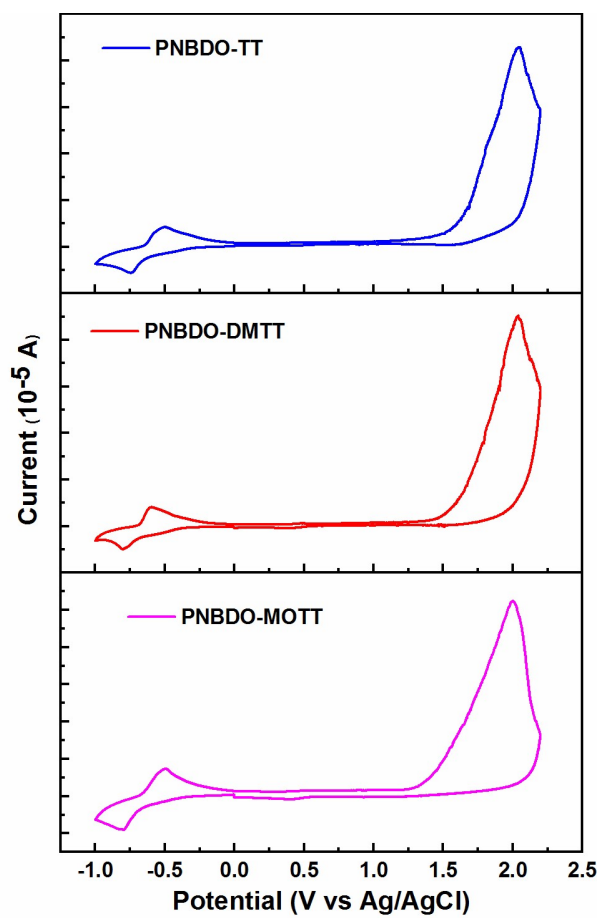


**Fig. S4** CV curves of PNBDO-TT, PNBDO-DMTT, and PNBDO-MOTT.

## 5. Theoretical modeling

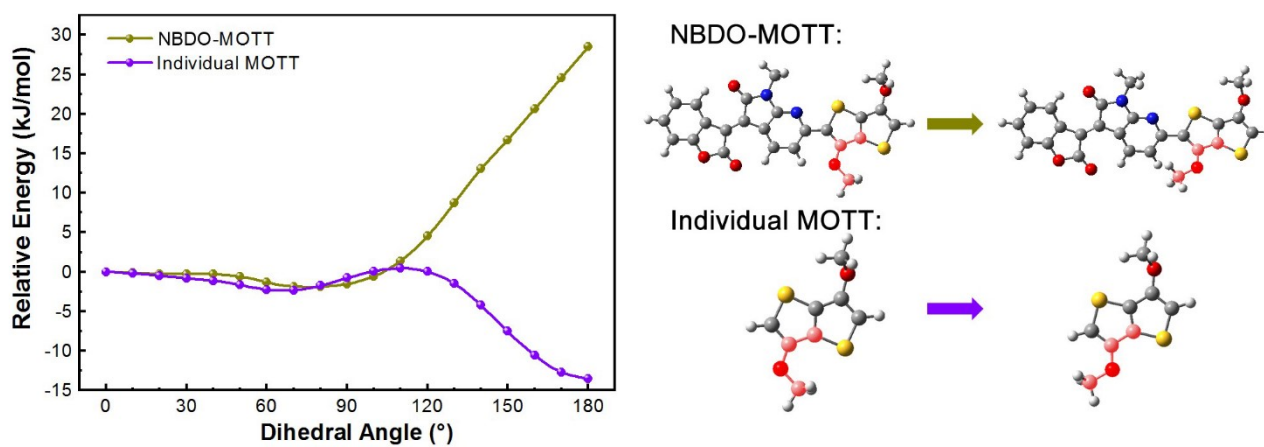


**Fig. S5** Potential energy distributions of **MOTT**-based subunit by rotation of the methoxy groups.

An individual **MOTT** unit was also studied for comparison. The single point energies were calculated at the MP2/ccpvdz level.

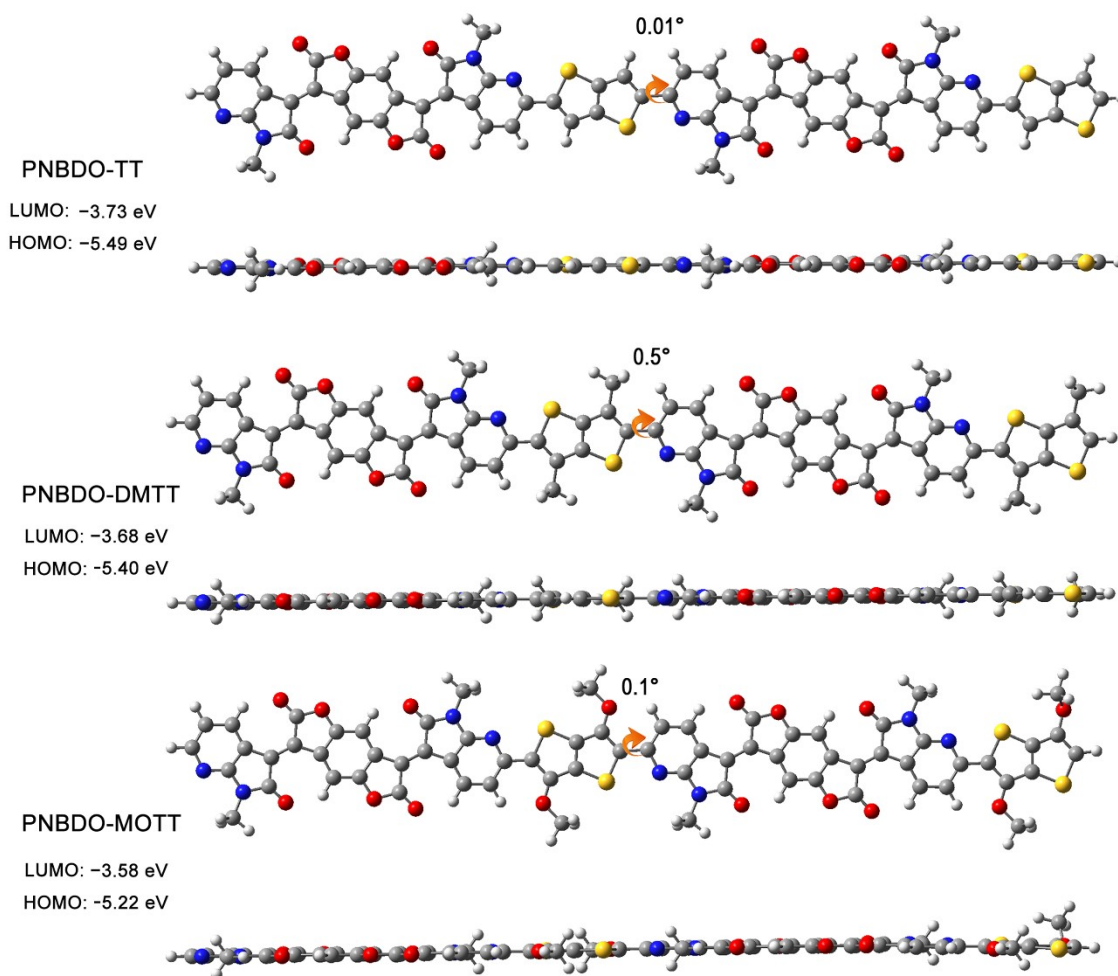


**Fig. S6** Optimized molecular geometries of **PNBDO-TT**, **PNBDO-DMTT**, and **PNBDO-MOTT** (dimers) using the density functional theory at the B3LYP/6-31G(d) level.

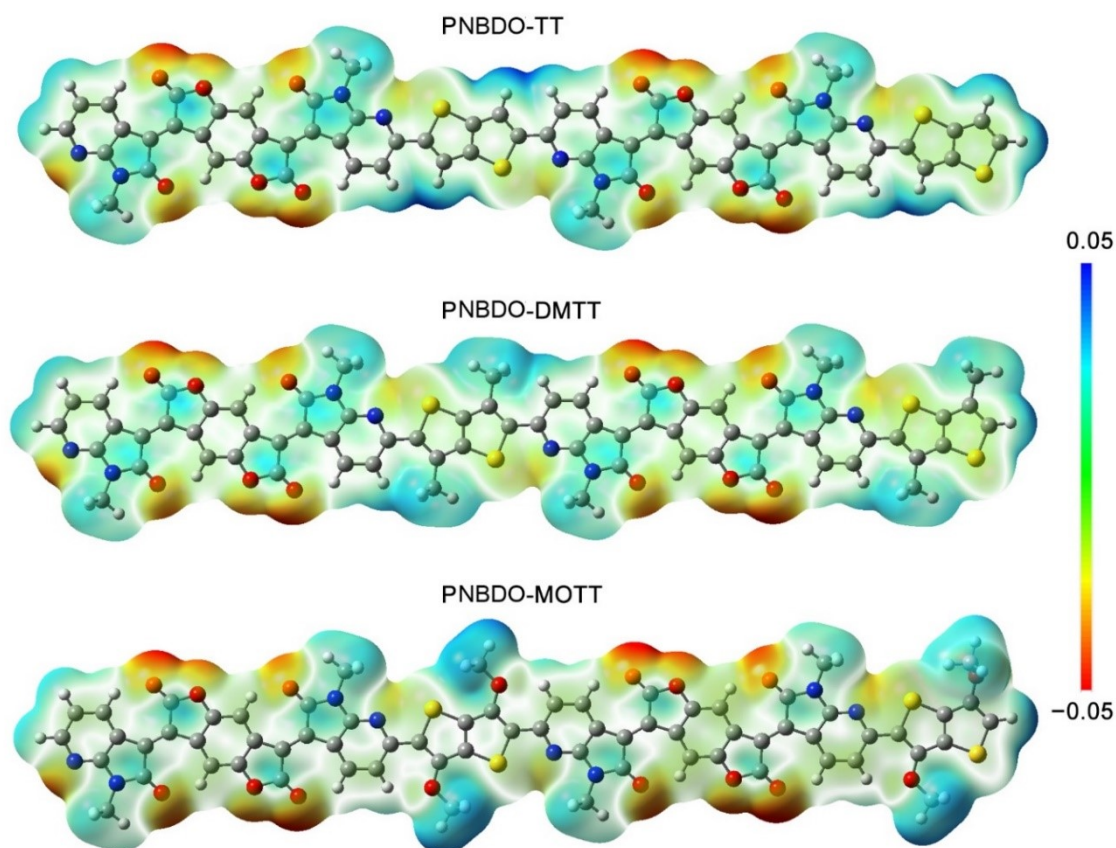


**Fig. S7** Electrostatic potential surface plots of **PNBDO-TT**, **PNBDO-DMTT**, and **PNBDO-MOTT** (dimers) at isovalue = 0.001 au.

**Figs. S7–S9** illustrate reduced density gradient versus sign ( $\lambda_2$ ) $\rho$  plots of **NBDO-TT**, **NBDO-DMTT**, and **NBDO-MOTT** subunits. The low-gradient, low-density spikes show the noncovalent interactions. Note that the attractions are negative, and their densities are larger than those of the competitive repulsions to stabilize the planar conformations. In all three subunits, considering the strength of attractions, the S...N conformation is the most stable local minimum.



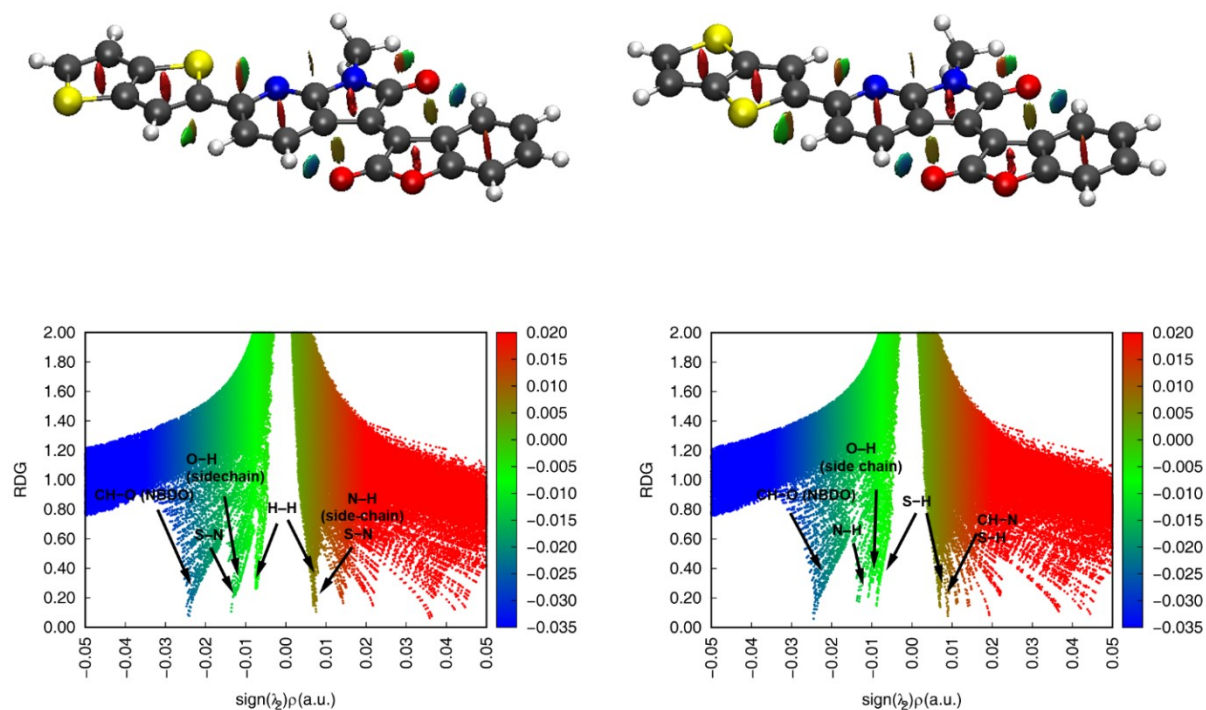


**Fig. S8** Reduced density gradient analysis of the NBDO–TT subunit.

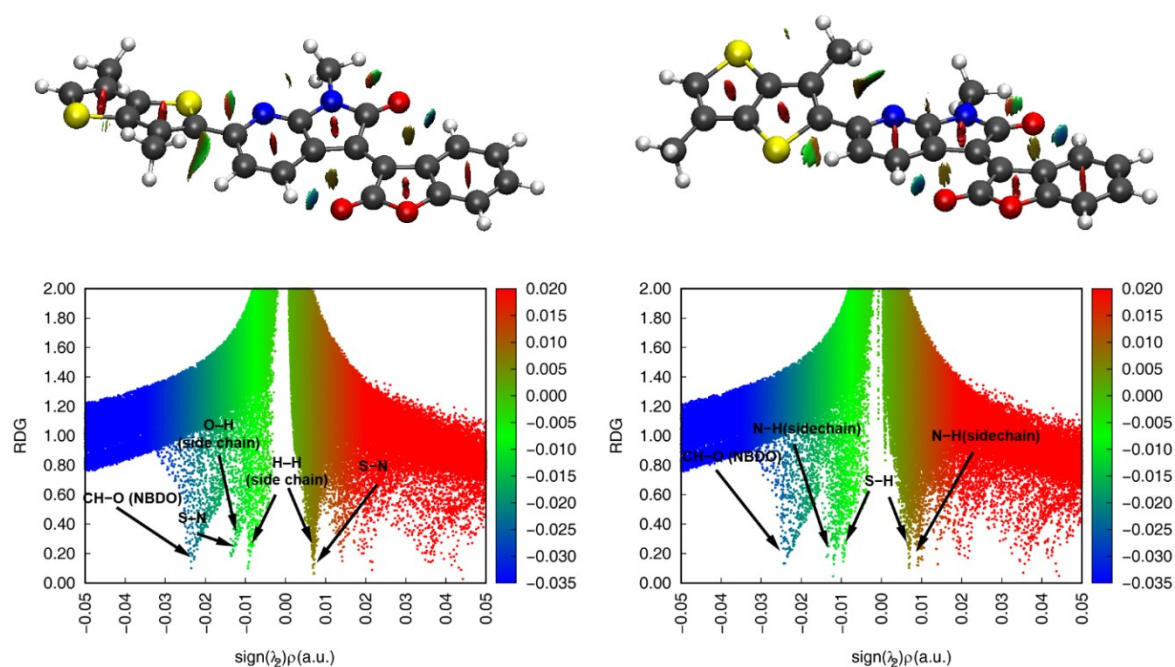


**Fig S9** Reduced density gradient analysis of the NBDO–DMTT subunit.

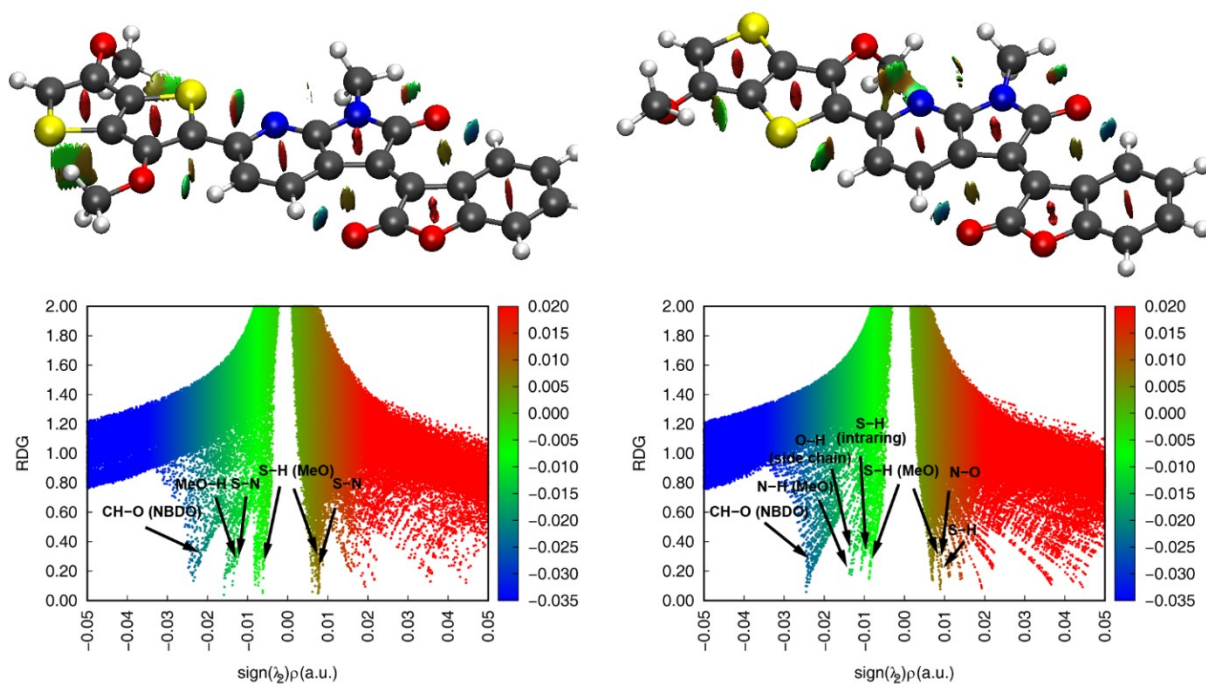


**Fig. S10** Reduced density gradient analysis of the **NBDO-MOTT** subunit.

## 6. Annealing temperature-dependent mobilities of PNBDO-TT

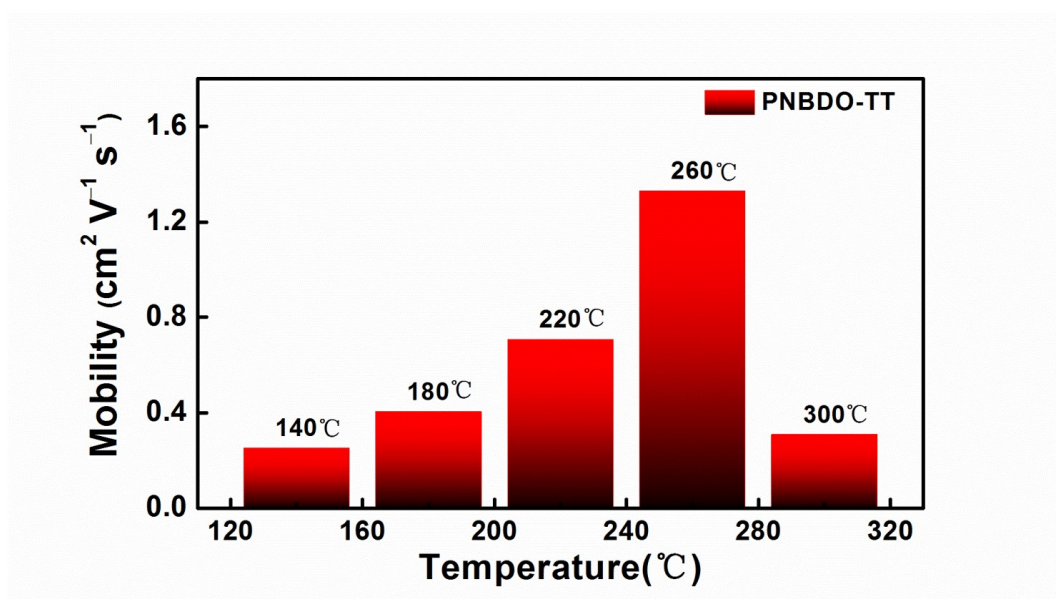


**Fig. S11** Annealing temperature-dependent mobilities of **PNBDO-TT**-based FET device.

## 7. Thin film morphology and aggregation characterizations

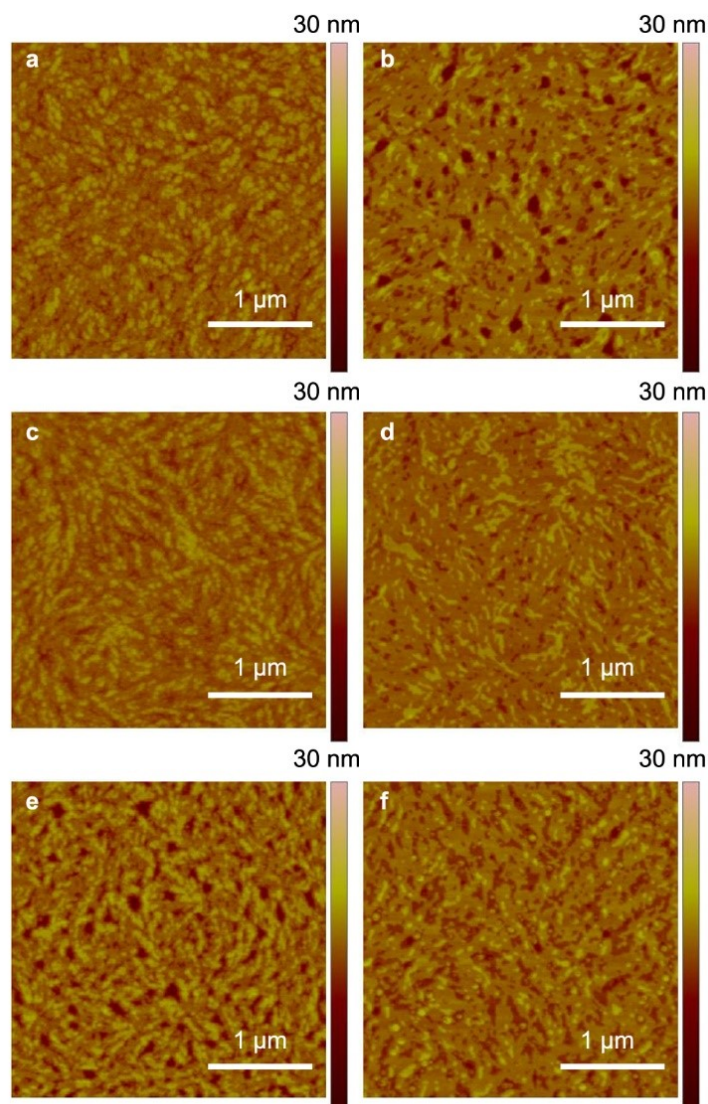


**Fig. S12** AFM images of polymer thin films in as-spun (a, c, e) and annealed thin films (b, d, f): (a, b) PNBDO-TT, (c, d) PNBDO-DMTT, and (e, f) PNBDO-MOTT.

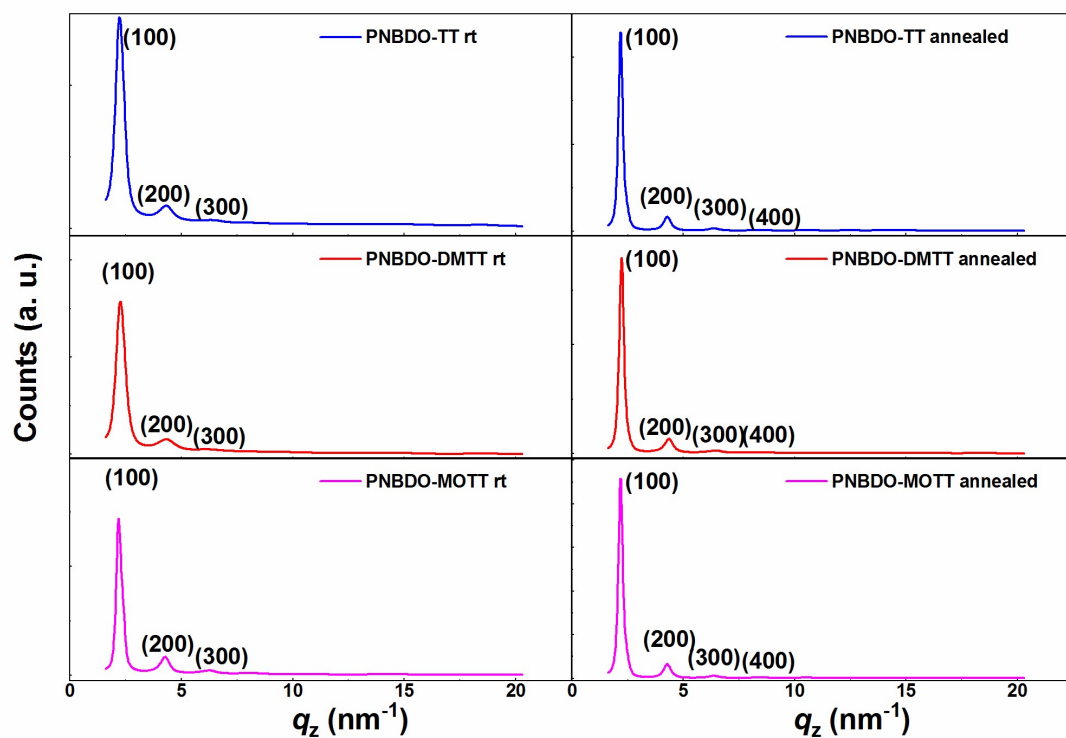


**Fig. S13** 1D Out-of-plane diffraction patterns of polymer thin films extracted from GIWAXS tests.

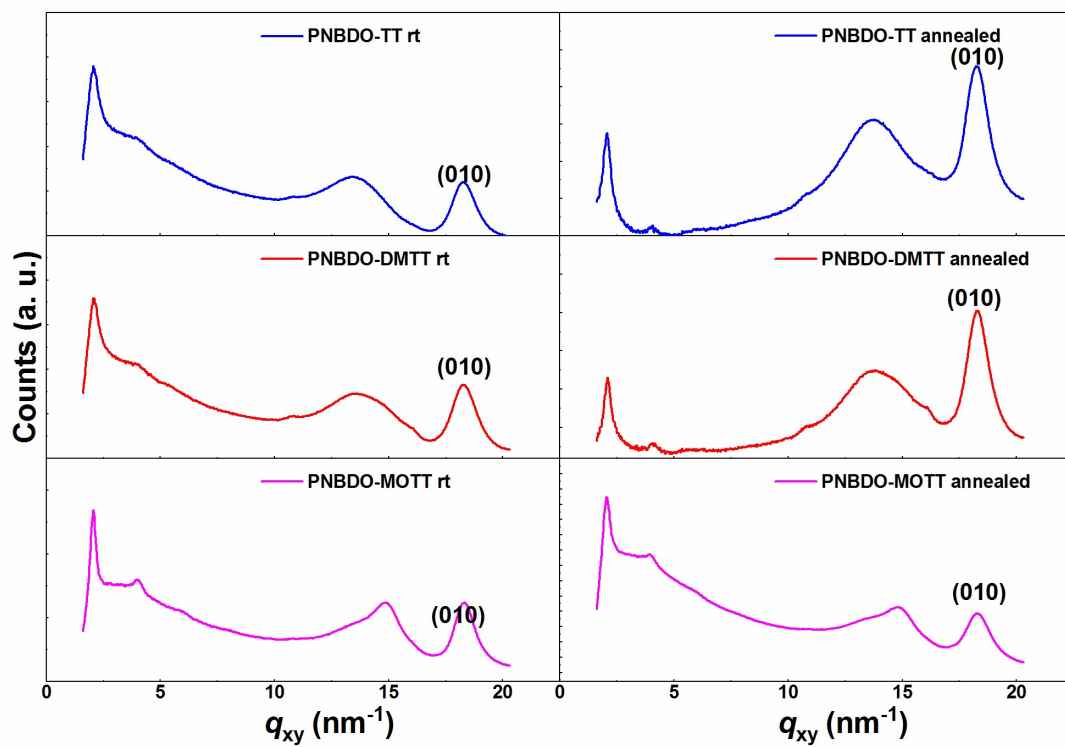


**Fig. S14** 1D In-plane diffraction patterns of polymer thin films extracted from GIWAXS tests.



## 8. NMR spectra of intermediates and polymers

